Supporting Information

Tuning Anionic Chemistry to Improve Kinetics of Mg Intercalation

Minglei Mao,†‡∥ Xiao Ji,†∥ Singyuk Hou,† Tao Gao,† Fei Wang,† Long Chen,† Xiulin Fan,† Ji Chen,† Jianmin Ma,‡ Chunsheng Wang*†

†Department of Chemical and Biomolecular Engineering, University of Maryland, College Park, Maryland 20742, United States

‡State Key Laboratory of Chemo/Biosensing and Chemometrics, School of Physics and Electronics, Hunan University, Changsha 410082, China

*Correspondence: cswang@umd.edu

Experimental section

Materials preparation

TiS_2 was purchase from Sigma Aldrich.

Preparation of $TiSe_2$: Layered $TiSe_2$ were prepared with a typical solid state method previously reported with slight modification.[1] Ti powder and slight excesses of Se powder were grounded and sealed in an evacuated quartz tube along with a small amount of iodine. The mixture was heated to 600 °C for 6 h, maintained in the temperature for 3 days, then naturally cooled to room temperature.

Preparation of VS_2: layered VS_2 were prepared via a simple hydrothermal method with some modifications.[2] 4 mmol NH_4VO_3 was dissolved in 60 ml deionized water and 5 mL $NH_3.H2O$ in a glass jar. Then, 30 mmol thioacetamide (TAA) was added with stirring for 0.5 h. Then, the solution was transferred to a 80 mL Teflon-lined sealed autoclave and maintained at 200℃ for 20 h. After that, the system was naturally cooled down to room temperature.

Preparation of VSe_2: Similar to $TiSe_2$, the solid state method was applied to prepare VSe_2 without iodine.[3]

Material Characterizations:

Hitachi (Tokyo, Japan) SU-70 HR-SEM was used to characterize the morphologies and size of the synthesized samples. X-ray powder diffraction (XRD) patterns were recorded on a Bruker Smart1000 diffractometer with a Cu Kα radiation. The Brunauer–Emmett–Teller (BET) measurements were carried out using a Micromeritics ASAP 2020 system.

Electrochemical Measurements:

Cell assembly was carried out in an Ar-filled glovebox with O_2 and H_2O levels below 0.1 ppm. TiS_2, $TiSe_2$, VS_2, and VSe_2 electrodes were prepared by compressing the as-prepared powders, PTFE, carbon black at a weight ratio of 8:1:1 onto the stainless steel grid. Electrochemical performance was tested in coin cells (2032), with APC electrolyte, polished Mg metal as the anode, and Celgard 2400 microporous polypropylene membrane as separators. The electrochemistry was conducted on Arbin battery test station (BT2000, Arbin Instruments, USA) at 5 mA/g with voltage cutoff of 0.5-2 V, with cells held in a thermostatted oven at room temperature. During GITT measurement, the electrode was discharged/charged at a pulse current of 5 mA/g for a duration of 2 h, followed by a relaxation of 5h at open circuit to reach equilibrium potentials. Nyquist plots were recorded using a Gamry 1000E electrochemical workstation (Gamry Instruments, USA) at a frequency range of 0.01-100 kHz.

The theoretical capacity of $TiSe_2$ ($C_{theoretical}$= 130 mA h/g) is calculated by:

$$C_{theoretical} = \frac{nF}{3.6M}$$
$$= \frac{1*96485}{3.6*205.79} mAh/g$$
$$= 130\ mAh/g$$

n is the number of electron transferred (n=1). F is the Faraday's constant (F=96485 C/mol). M is the relative molecular mass (M=205.79 g/mol). Similarly, the theoretical capacity of VSe_2 is 128 mA h/g.

The electrical conductivity of hosts is calculated by

$$R = \rho\frac{L}{A}$$

$$\sigma = \frac{1}{\rho}$$

ρ is the resistivity. R is the resistance. L is the length of hosts along the direction of the current. A is the cross-sectional area. σ is the electrical conductivity of the hosts.

First Principles Calculations:

All first-principles computations based on density functional theory (DFT)[4, 5] are performed using the Vienna ab initio Simulation Package (VASP) package. The Projector Augmented Wave (PAW)[6] method with an energy cut-off of 520 eV is used to describe the ion-electron interaction on a well-converged k-point mesh. The Perdew-Burke-Ernzerhof (PBE) functional in the Generalized Gradient Approximation (GGA)[7] is employed to calculate the exchange-correlation energy. The DFT-D3 is used to correct van der Waals energy to get accurate interlayer spacing values.[8] Layered VO_2 and TiO_2 are constructed based on the structure of VS_2 and TiS_2 and then optimized the lattice parameters and atomic position. The geometry optimizations are performed using the conjugated gradient method, and the convergence threshold is set to be 10-5 eV in energy and 0.01 eV/Å in force. Furthermore, the climbing image nudged elastic band (CINEB) method implemented in VASP is used to determine the diffusion barriers.[9] Visualization of the atomic structures are made by using VESTA software.[10] The isosurfaces plots of charge distribution for Mg intercalated electrode materials (MX_2) are obtained by subtracting charge densities of Mg and MX_2 from that of Li Mg intercalated MX_2, i.e. $\Delta\rho=\rho(MgMX_2)-\rho(Mg)-\rho(MX_2)$

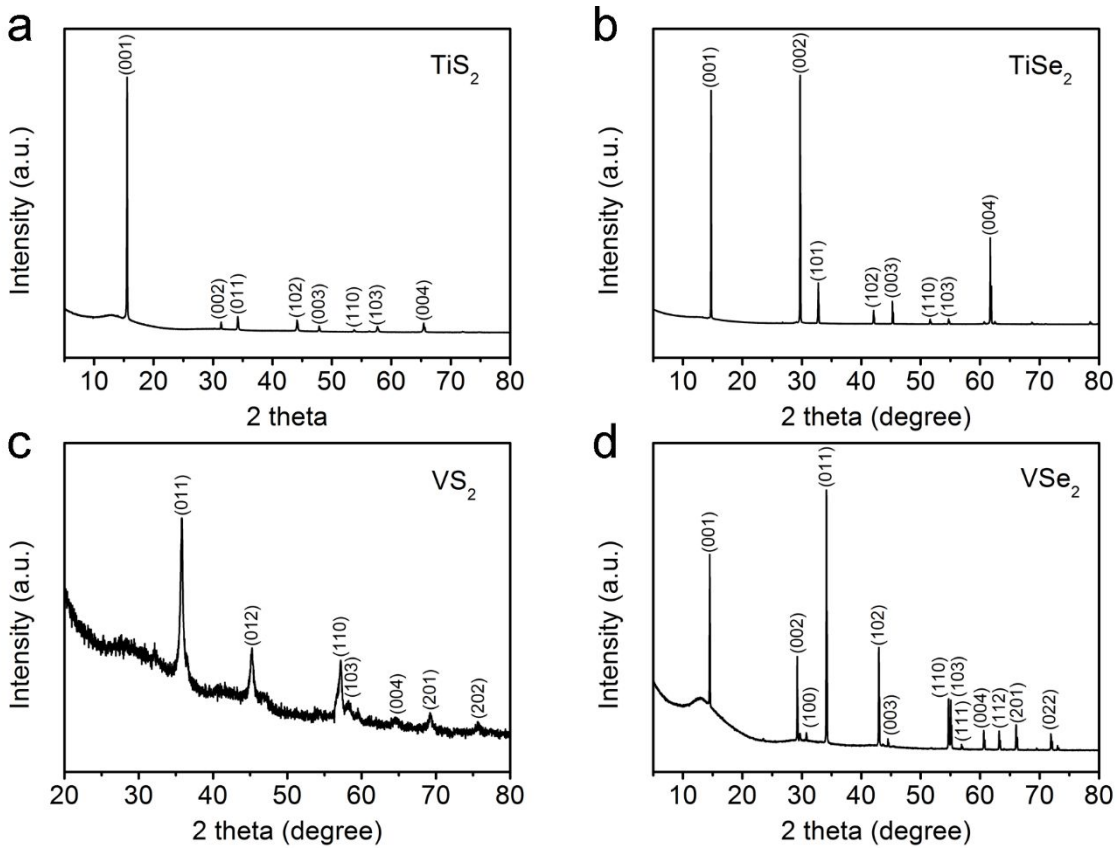

Figure S1. (a-d) XRD of trigonal TiS_2, $TiSe_2$, VS_2, and VSe_2 powder, respectively. All the peaks correspond to the standard PDF #88-2479, #83-0980, #89-1640, and #89-1641, respectively.

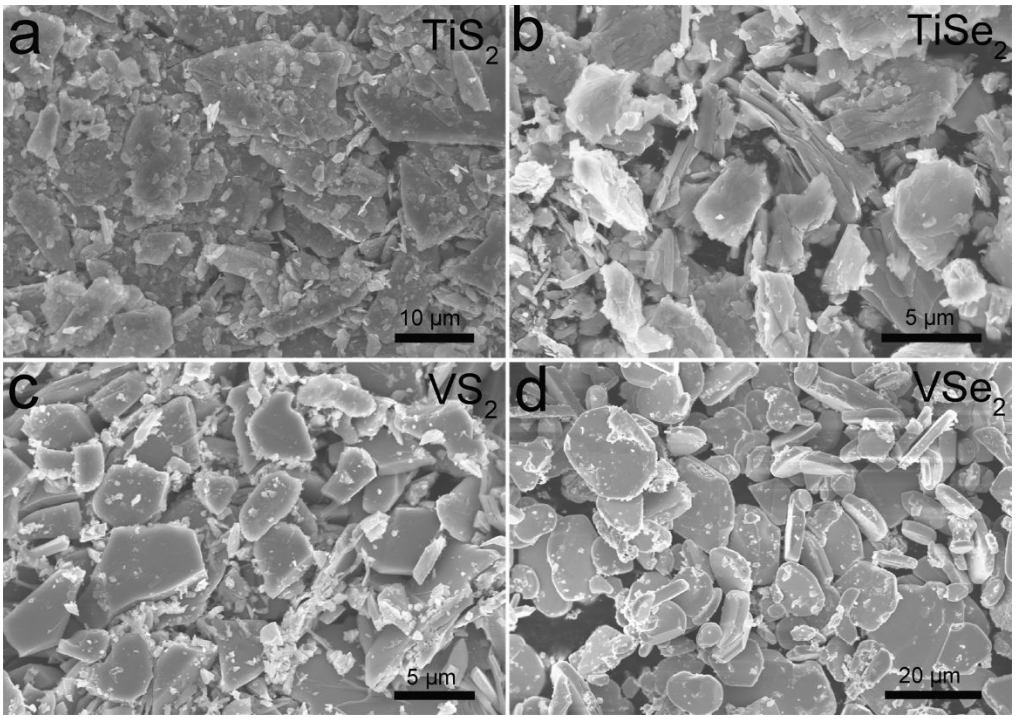

Figure S2. (a-d) SEM of TiS_2, $TiSe_2$, VS_2, and VSe_2, respectively. The particle sizes of these four compounds are 2-20 μm, 2-10 μm, 1-10 μm, and 5-20 μm, respectively.

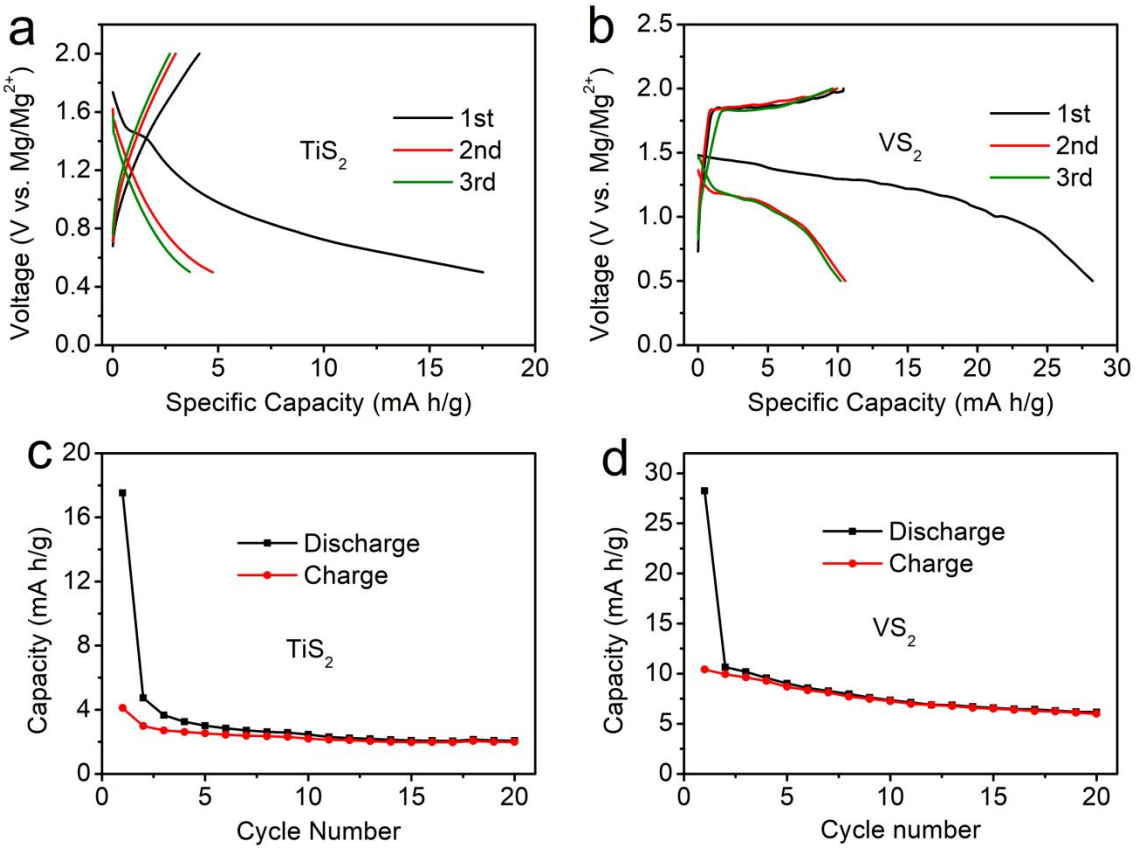

Figure S3. The discharge-charge curves of (a) TiS_2 and (b) VS_2 for the first three cycles. (c-d) Cycling performance of (c) TiS_2 and (d) VS_2 with APC electrolyte and metal Mg anode between 0.5 and 2 V at the current density of 5 mA/g under room temperature.

.

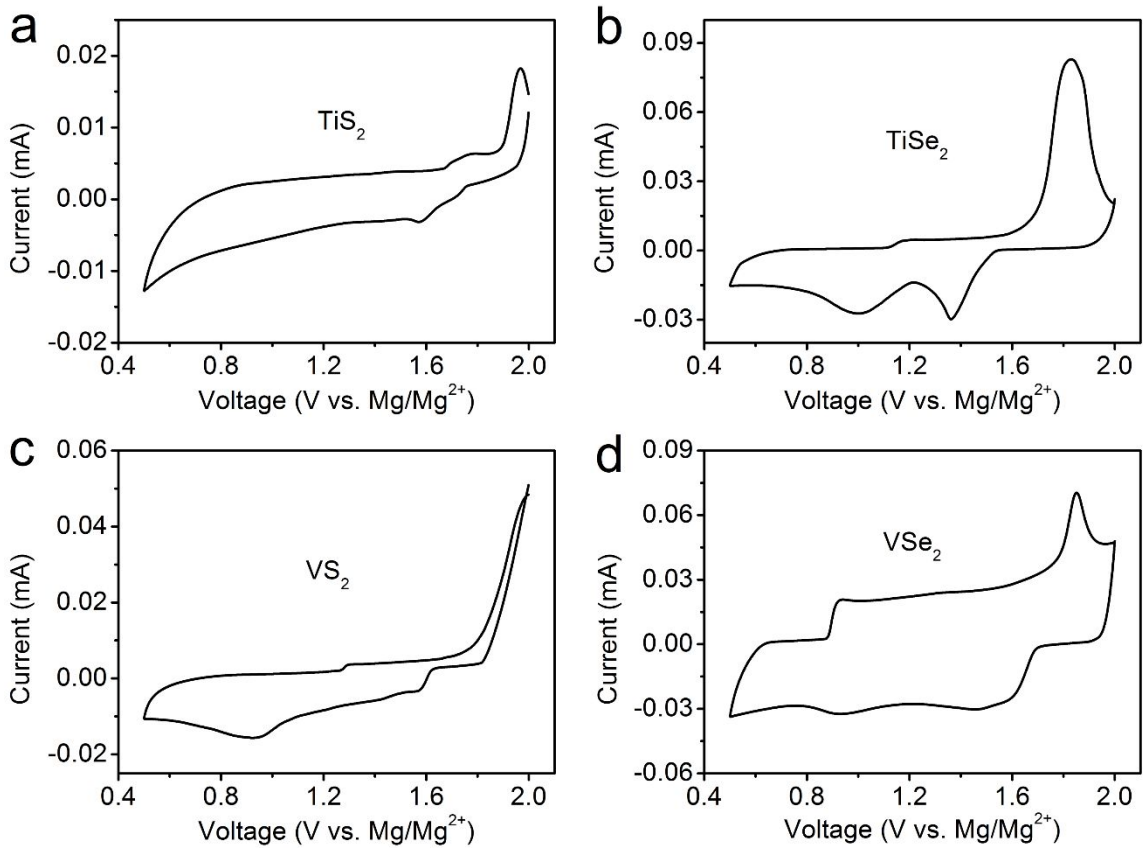

Figure S4. CV profiles of (a) TiS_2, (b) $TiSe_2$, (c) VS_2, and (d) VSe_2 at sweep rate of 0.2 mV/s.

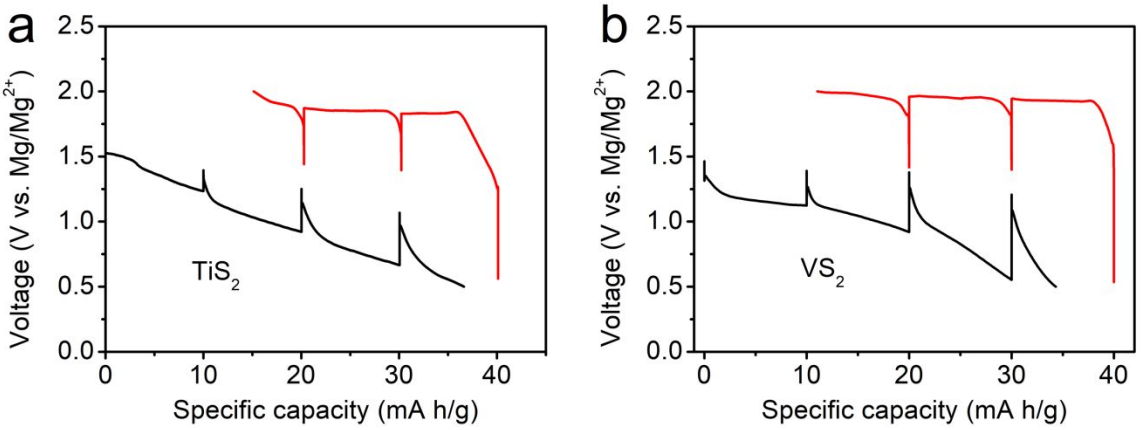

Figure S5. Quasi-equilibrium voltage profile of (a) TiS_2 and (b) VS_2 obtained from GITT. The cells were allowed to relax for 5 h after every 2 h discharging or charging at 5 mA/g at RT.

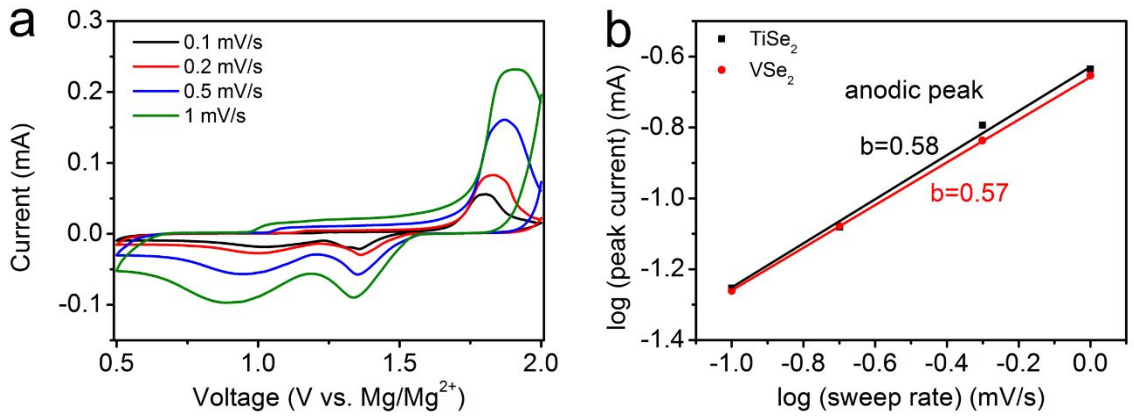

Figure S6. (a) Cyclic voltammograms of $TiSe_2$ at different sweep rate in the range of 0.1-1 mV/s. (b) The log(i) versus log(v) plot of the anodic current response at ~1.8V (versus Mg/Mg2+). The slope of this line gives the b value, which shows that this value is close to 0.58 for $TiSe_2$ and 0.57 for VSe_2.

The resistance values for sulfides and selenides at open-circuit voltage states (OCV), fully discharged states (0.5 V), and fully charged states (2 V) obtained from fitting are listed in Table S1, in which the electrolyte resistance (Rs) for Ti or V sulfide and selenide are comparable at different states. The total surface resistance (R1+R2) for Ti or V sulfide are always much higher than the selenide.

Table S1. Electrode resistances for sulfides and selenides at open-circuit voltage states (OCV), fully discharged states (0.5 V), and fully charged states (2V) obtained from equivalent circuit fitting of EIS results.

	TiS2			TiSe2			VS2			VSe2		
	OCV	0.5V	2V	OCV	0.5V	2V	OCV	0.5V	2V	OCV	0.5V	2V
Rs	70	75.66	77.44	93.01	48.59	44.78	95.5	184	190	60.87	35.5	194
R1	2100	4025	7904	293.6	1212	1246	522	1647	2579	395.3	664.2	1004
R2	1600	4845	3398	2933	7690	3150	1480	4527	4880	4688	8200	6000

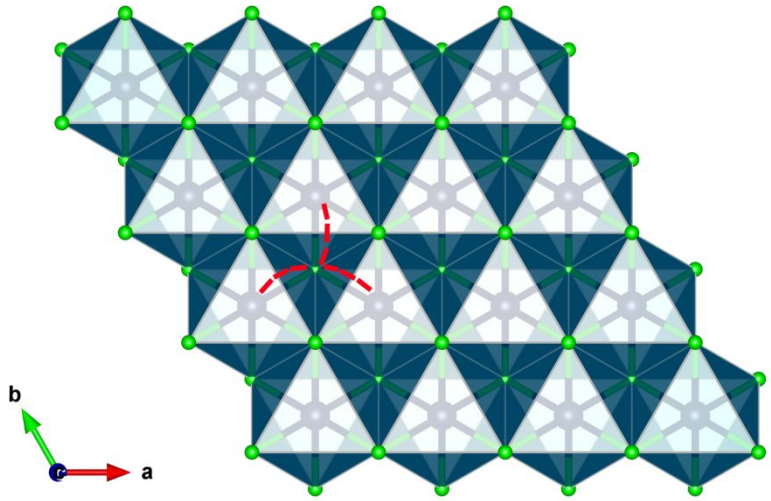

Figure S7. Top view of the crystal structure of layered MX_2 (M=Ti, V; X=O, S, Se). Ti or V atoms (dark blue) are at the center of octahedra constructed of X atoms (green). Mg^{2+} migrates between the empty interlayer octahedral sites through the intermediate tetrahedral sites, which is marked in red dashed line.

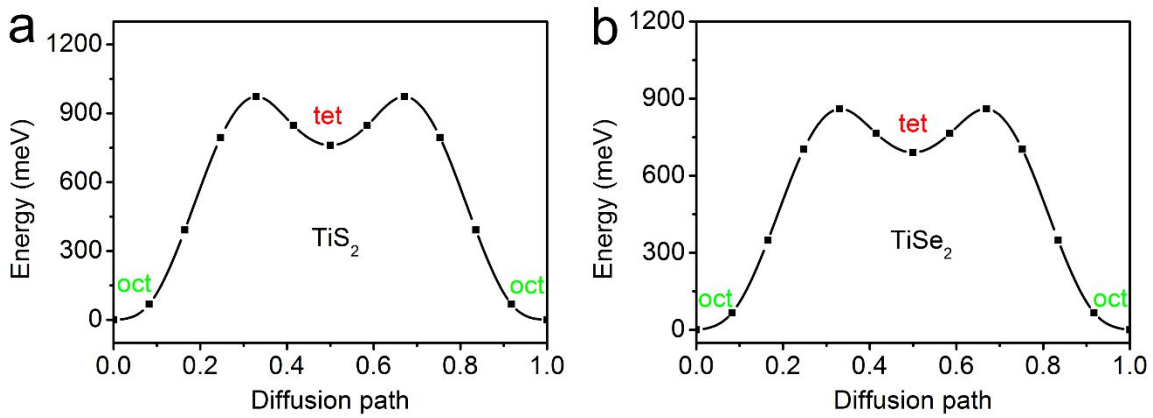

Figure S8. Calculated energy barrier for migration of Mg^{2+} in layered structure along the minimum energy path as obtained by first-principles nudged elastic band (NEB) in calculations. (a) TiS_2 and (b) $TiSe_2$ within dilute limit of cation insertion.

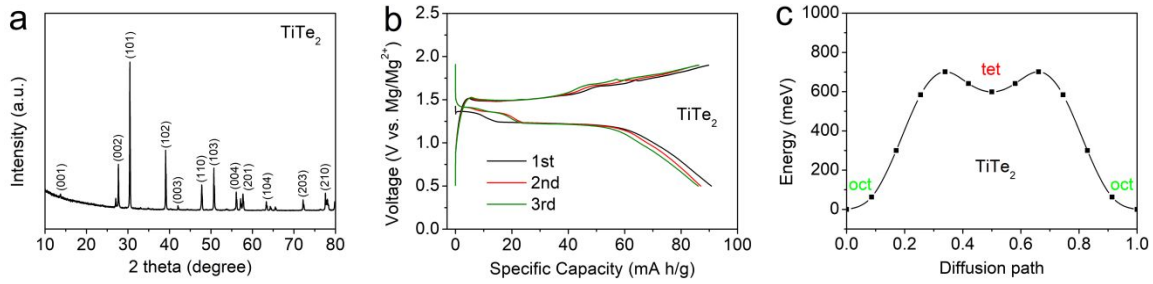

Figure S9. (a) XRD of $TiTe_2$. All the peaks correspond to the standard PDF #32-1388. (b) The discharge-charge curves of $TiTe_2$ for the first three cycles, with APC electrolyte and metal Mg anode between 0.5 and 2 V at the current density of 5 mA/g under room temperature. (c) Calculated energy barrier for migration of Mg^{2+} in $TiTe_2$ along the minimum energy path as obtained by first-principles nudged elastic band (NEB) in calculations.

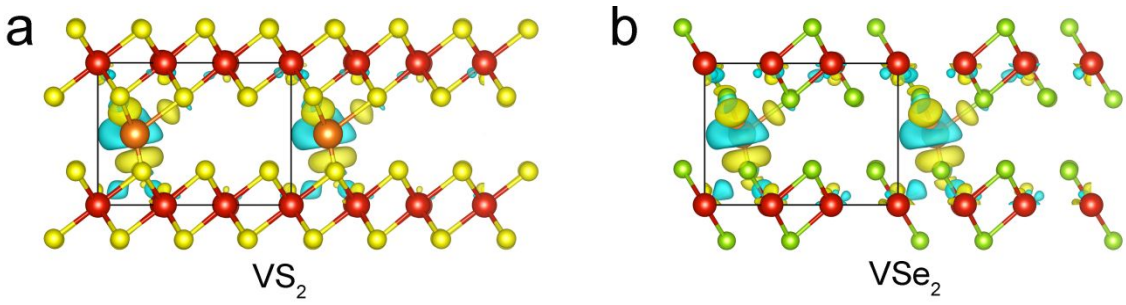

Figure S10. Charge rehybridization upon diffusion of Mg^{2+} between layers of (a) VS_2 and (b) VSe_2 at the energetic maxima. Areas of charge accumulation are shown in yellow while depletion is shown in blue. Sulfur as small yellow spheres, selenium as small kelly spheres, V as big green spheres, and Mg at the center as an orange sphere.

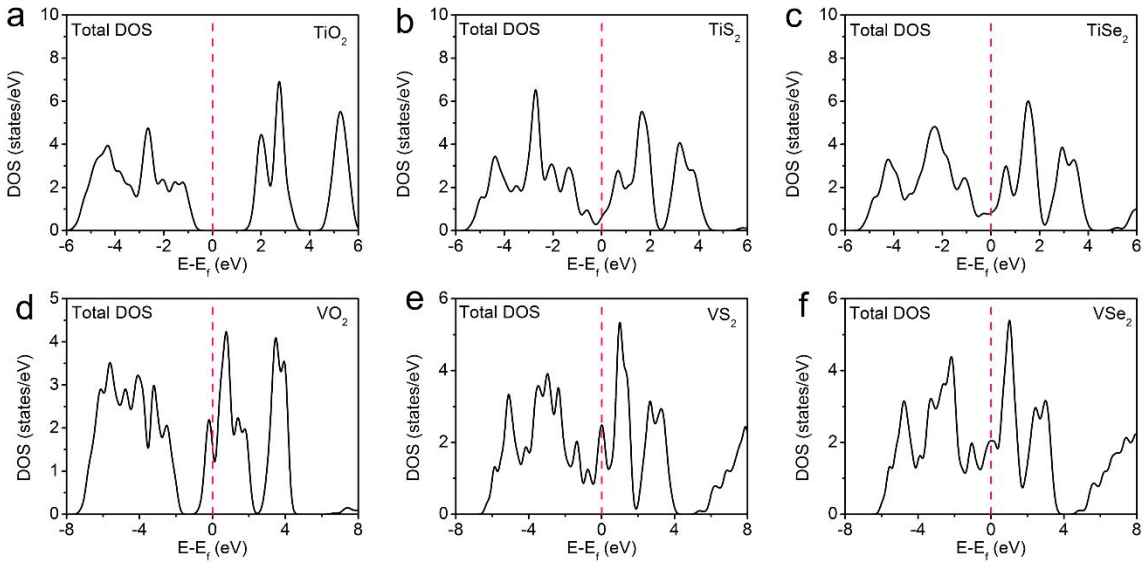

Figure S11. Total density of states (DOS) for layered (a) TiO_2, (b) TiS_2, (c) $TiSe_2$, (d) VO_2, (e) VS_2, and (f) VSe_2.

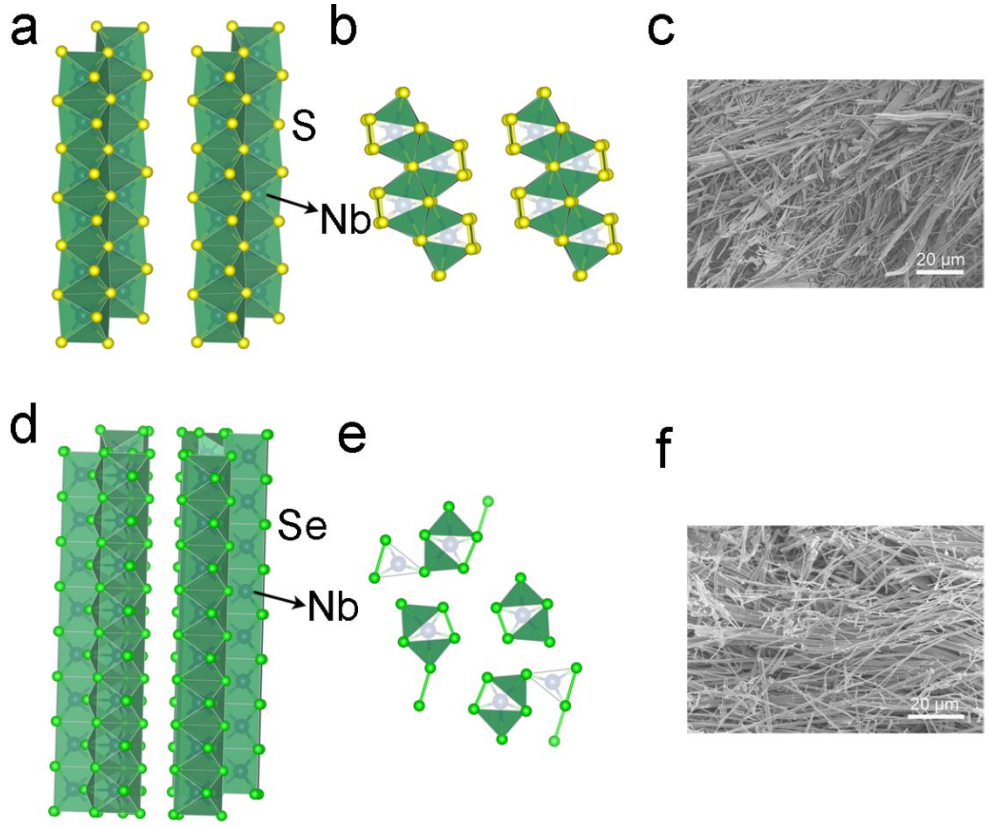

Figure S12. (a, d) Crystal structure, (b, e) project of the crystal structure along [010]-axis and [100]-axis, and (c, f) SEM of triclinic NbS_3 and monoclinic $NbSe_3$, respectively.

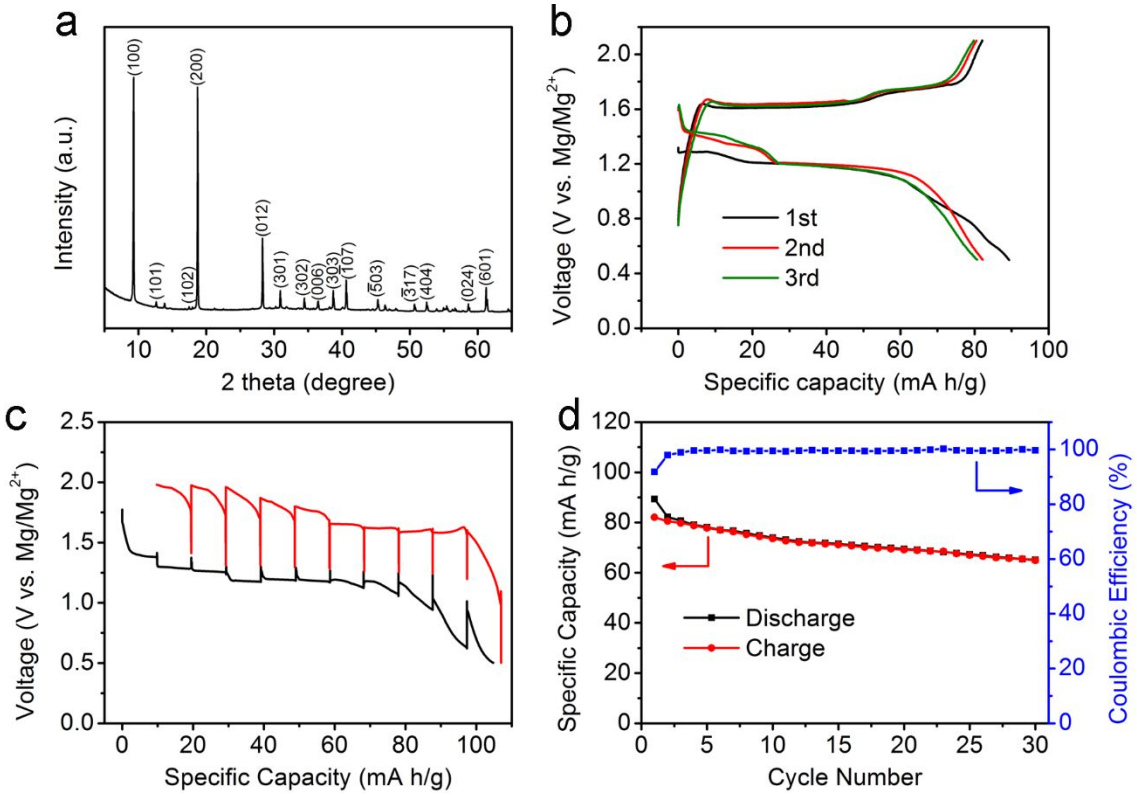

Figure S13. XRD and electrochemical performance of monoclinic $NbSe_3$. (a) XRD of monoclinic $NbSe_3$ powder. All the peaks correspond to the standard PDF #75-0763. (b-c) The first three discharge-charge curves, GITT, and cycling performance of $NbSe_3$, respectively, with APC electrolyte and Mg anode between 0.5 and 2 V at 5 mA/g and RT.

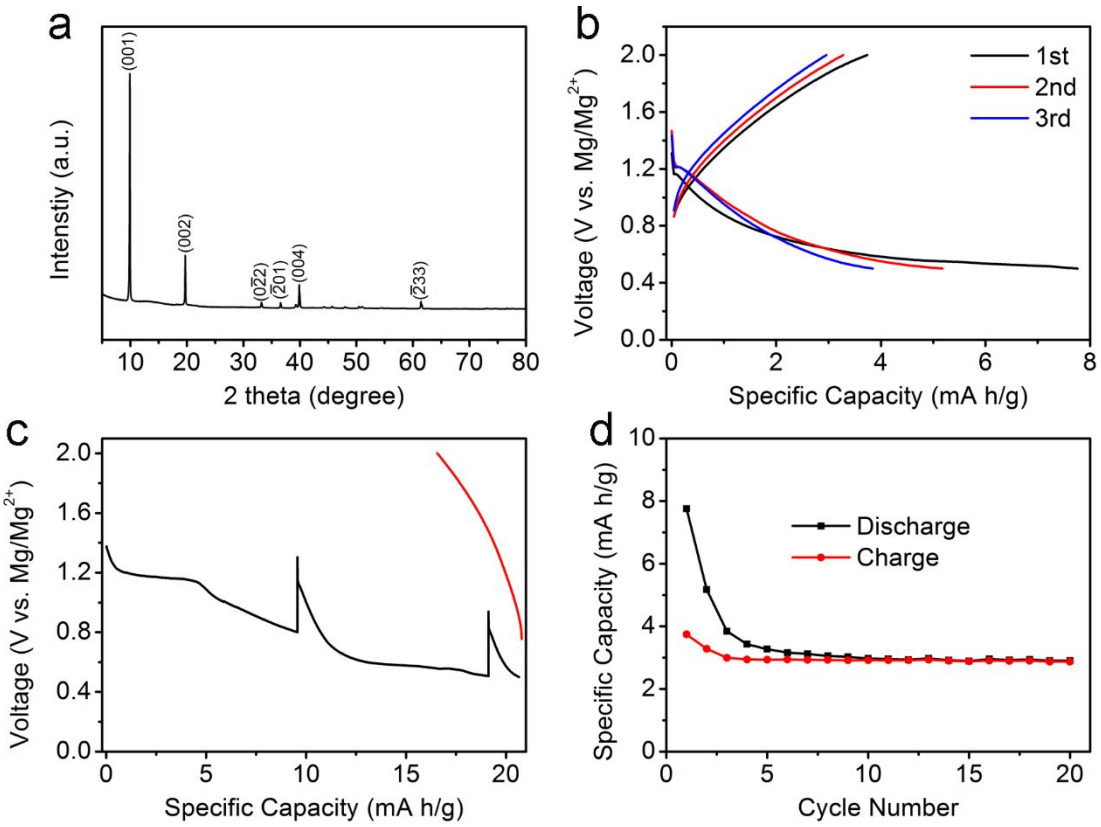

Figure S14. XRD and electrochemical performance of triclinic NbS_3. (a) XRD of triclinic $NbSe_3$ powder. All the peaks correspond to the standard PDF #71-0468. (b-c) The first three discharge-charge curves, GITT, and cycling performance of NbS_3, respectively, with APC electrolyte and Mg anode between 0.5 and 2 V at 5 mA/g and RT.

Reference

1. Y. I. Joe, X. M. Chen, P. Ghaemi, K. D. Finkelstein, G. A. de la Peña, Y. Gan, J. C. T. Lee, S. Yuan, J. Geck, G. J. MacDougall, T. C. Chiang, S. L. Cooper, E. Fradkin and P. Abbamonte. Emergence of charge density wave domain walls above the superconducting dome in 1T-TiSe2. Nature Physics, 2014, 10, 421.
2. H. Pan, Y. Mengyu, Z. Guobin, S. Ruimin, C. Lineng, A. Qinyou and M. Liqiang. Layered VS2 Nanosheet - Based Aqueous Zn Ion Battery Cathode. Advanced Energy Materials, 2017, 7, 1601920.
3. A. H. Thompson, J. C. Scanlon and C. R. Symon. The electrochemical reaction of Li with VSe2 and implications on the ionicity of intercalation compounds. Solid State Ionics, 1980, 1, 47-57.
4. P. Hohenberg and W. Kohn. Inhomogeneous Electron Gas. Physical Review, 1964, 136, B864-B871.
5. W. Kohn and L. J. Sham. Self-Consistent Equations Including Exchange and Correlation Effects. Physical Review, 1965, 140, A1133-A1138.
6. P. E. Blöchl. Projector augmented-wave method. Physical Review B, 1994, 50, 17953-17979.
7. J. P. Perdew, K. Burke and M. Ernzerhof. Generalized Gradient Approximation Made Simple. Phys. Rev. Lett., 1996, 77, 3865-3868.
8. A consistent and accurate ab initio parametrization of density functional dispersion correction (DFT-D) for the 94 elements H-Pu. The Journal of Chemical Physics, 2010, 132, 154104.
9. A climbing image nudged elastic band method for finding saddle points and minimum energy paths. The Journal of Chemical Physics, 2000, 113, 9901-9904.
10. K. Momma and F. Izumi. VESTA 3 for three-dimensional visualization of crystal, volumetric and morphology data. Journal of Applied Crystallography, 2011, 44, 1272-1276.